Conception of a prompt gamma detector for the hadrontherapy online monitoring

Maxime Jacquet

Supervisor: Marie-Laure Gallin-Martel
Co-supervisor: Sara Marcatili

Laboratoire de Physique Subatomique et Cosmologie

1. Introduction
2. New imaging modality: Prompt Gamma Time Imaging
3. Conception of TIARA detection system
   - Crystal optimization
   - Photodetector characterization
4. Conclusion

1. Introduction
2. New imaging modality: Prompt Gamma Time Imaging
3. Conception of TIARA detection system
   - Crystal optimization
   - Photodetector characterization
4. Conclusion

Proton therapy

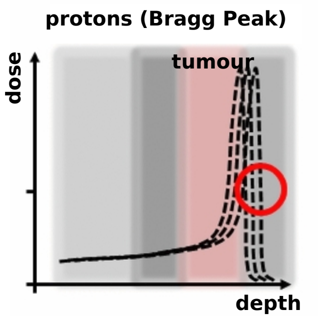

Knopf et al 2013 Phys. Med. Biol. 58 R131

Maximal energy deposition nearby the end of the proton range

⇒ Possibility of a **high ballistic precision**

Proton therapy

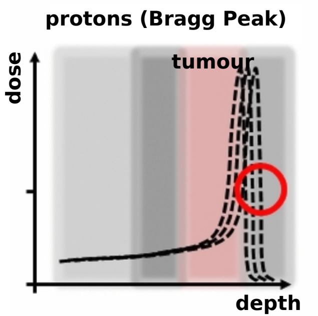

Knopf et al 2013 Phys. Med. Biol. 58 R131

Maximal energy deposition nearby the end of the proton range

$\Rightarrow$ Possibility of a **high ballistic precision**

Uncertainties on the proton range

$\Rightarrow$ Establishment of safety margins

Proton therapy

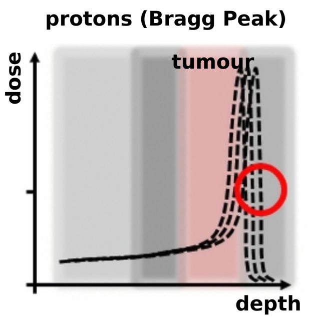

Knopf et al 2013 Phys. Med. Biol. 58 R131

Maximal energy deposition nearby the end of the proton range

$\Rightarrow$ Possibility of a **high ballistic precision**

Uncertainties on the proton range

$\Rightarrow$ Establishment of safety margins

Online proton therapy monitoring

- Detection of **secondary particles** coming from nuclear collisions
- Location of the **Bragg Peak** in real time
- Reduction of the applied safety margins

  $\Rightarrow$ Improvement of treatment accuracy

Proton therapy

protons (Bragg Peak)

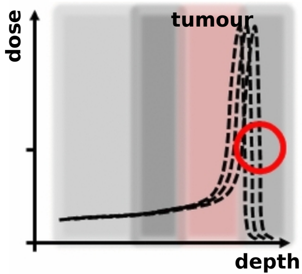

Knopf et al 2013 Phys. Med. Biol. 58 R131

Maximal energy deposition nearby the end of the proton range

⇒ Possibility of a **high ballistic precision**

Uncertainties on the proton range

⇒ Establishment of safety margins

Online proton therapy monitoring

- Detection of **secondary particles** coming from nuclear collisions
- Location of the **Bragg Peak** in real time
- Reduction of the applied safety margins

  ⇒ Improvement of treatment accuracy

Secondary particles studied: **Prompt Gamma (PG)**

Prompt Gamma

Prompt gamma:

Gamma emitted by a nuclear de-excitation following a nuclear collision within the target

PG features

- $1 < E_{P_G} < 8$ MeV
- $\approx$ Isotropic emission
- ✓ $\langle T_{PG} \rangle < 1$ ps
- ✗ Low available statistics : $\approx$ **0.01** $\gamma.p^{-1}.cm^{-1}$

Prompt Gamma

Prompt gamma:

Gamma emitted by a nuclear de-excitation following a nuclear collision within the target

PG features

- $1 < E_{P_G} < 8$ MeV
- $\approx$ Isotropic emission
- ✓ $\langle T_{PG} \rangle < 1$ ps
- ✗ Low available statistics : $\approx$ **0.01** $\gamma.p^{-1}.cm^{-1}$

PG interesting properties

- **Spatial correlation** between PG emission profile and proton range

$\Rightarrow$ Short $\langle T_{PG} \rangle$ implies a **time correlation**

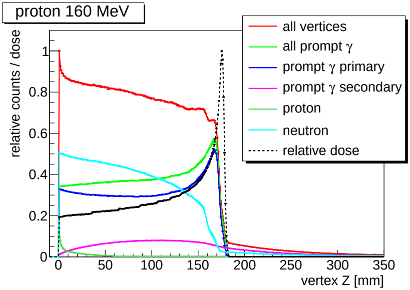

Krimmer et al, NIMA 2018

Prompt Gamma

Prompt gamma:

Gamma emitted by a nuclear de-excitation following a nuclear collision within the target

PG features

- $1 < E_{P_G} < 8$ MeV
- $\approx$ Isotropic emission
- ✓ $\langle T_{PG} \rangle < 1$ ps
- ✗ Low available statistics : $\approx$ **0.01** γ.p^{-1}.cm^{-1}

PG interesting properties

- **Spatial correlation** between PG emission profile and proton range

$\Rightarrow$ Short $\langle T_{PG} \rangle$ implies a **time correlation**

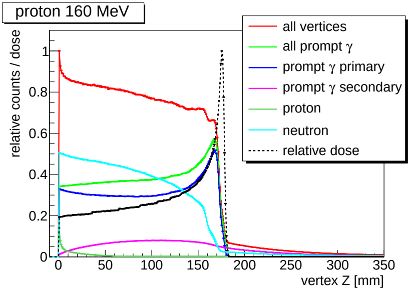

Krimmer et al, NIMA 2018

Time-Of-Flight(TOF)-based online monitoring

PG timing (PGT): concept

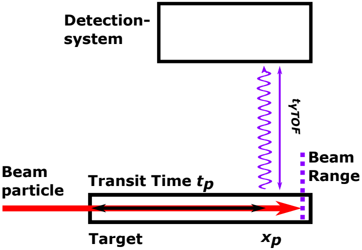

Golnik et al 2014 Phys. Med. Biol. 59 5399

PG timing (PGT): concept

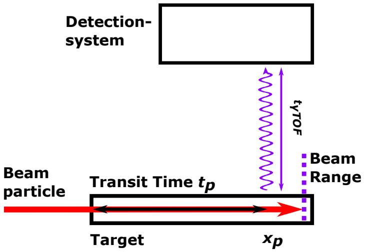

Golnik et al 2014 Phys. Med. Biol. 59 5399

Measurement of the $t_p + t_\gamma$ distribution

PGT features

- ✓ **Monitoring in real time**
- ✓ High detection efficiency
- ✓ Neutron rejection by TOF
- ✗ TOF limited by: the bunch width
  the beam instabilities

$\Rightarrow \approx$ **1 ns** rms of time resolution (cyclotron)

PG timing (PGT): concept

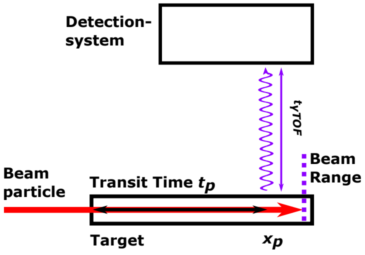

Golnik et al 2014 Phys. Med. Biol. 59 5399

Measurement of the $t_p + t_\gamma$ distribution

PGT features

- ✓ **Monitoring in real time**
- ✓ High detection efficiency
- ✓ Neutron rejection by TOF
- ✗ TOF limited by: the bunch width
  the beam instabilities

$\Rightarrow$ $\approx$ **1 ns** rms of time resolution (cyclotron)

Increase PGT sensitivity by means of a beam monitor in a single proton regime

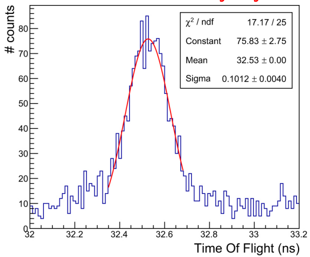

Marcatili et al 2020 Phys. Med. Biol. 65 245033

Increase of PGT sensitivity method

- Reduction of the beam current
- Beam monitor: diamond hodoscope
- **TOF** detection
  hodoscope - gamma detector

$\Rightarrow$ Coincidence time resolution: **101 ps** rms

Time of flight Imaging ArRAy (TIARA)

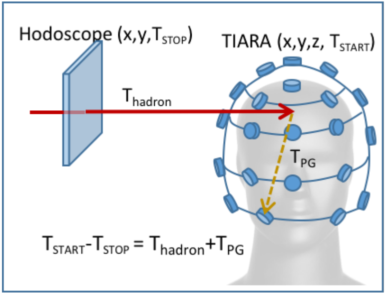

TIARA

PG detectors: PG TOF and hit position measured by $\approx$ 30 small-size pixels

Combination of:

$$\left.\begin{array}{l}\bullet\ \text{TIARA detectors}\\ \bullet\ \text{Beam monitor}\\ \bullet\ \text{Single proton}\end{array}\right\} \Rightarrow \approx \textbf{100 ps rms}$$

Time of flight Imaging ArRAy (TIARA)

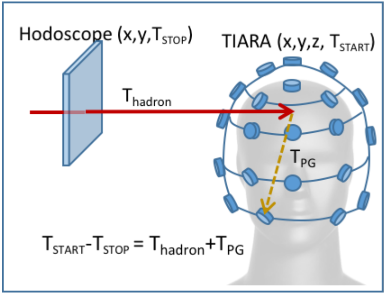

TIARA

PG detectors: PG TOF and hit position measured by ≈ 30 small-size pixels

Combination of:

- TIARA detectors
- Beam monitor
- Single proton

⇒ ≈ **100 ps rms**

TOF-based reconstruction of PG vertices: PG Time Imaging (PGTI) approach

Time of flight Imaging ArRAy (TIARA)

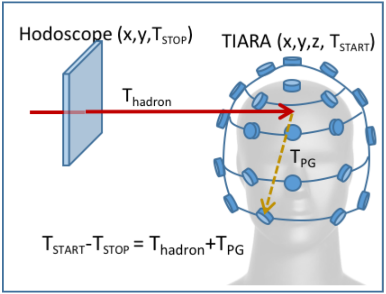

TIARA

PG detectors: PG TOF and hit position measured by ≈ 30 small-size pixels

Combination of:

- TIARA detectors
- Beam monitor
- Single proton

$\Rightarrow \approx$ **100 ps rms**

TOF-based reconstruction of PG vertices: PG Time Imaging (PGTI) approach

Vertex reconstruction

$$T_{Start} - T_{stop} = T_{proton}(\mathbf{r}_v) + \frac{1}{c}\|\mathbf{r}_d - \mathbf{r}_v\|$$

- $T_{PG}(\mathbf{r}_d,\mathbf{r}_v)$: Analytical determination
- $T_{proton}(\mathbf{r}_v)$: Monte Carlo (MC) simulation

Development and validation of the vertex reconstruction method + 1D approximation

1 Introduction

2 New imaging modality: Prompt Gamma Time Imaging

3 Conception of TIARA detection system
- Crystal optimization
- Photodetector characterization

4 Conclusion

Validation of reconstruction method

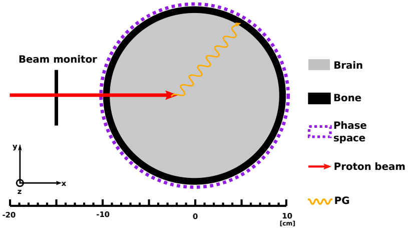

Simulated geometry (GEANT4.10.4 release)

- A 10 cm radius head
- A diamond-based beam hodoscope placed 5 cm upstream the head
- A phase space surrounding the head
- 100 MeV proton beam

Validation of reconstruction method

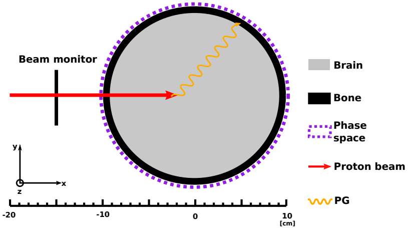

Simulated geometry (GEANT4.10.4 release)

- A 10 cm radius head
- A diamond-based beam hodoscope placed 5 cm upstream the head
- A phase space surrounding the head
- 100 MeV proton beam

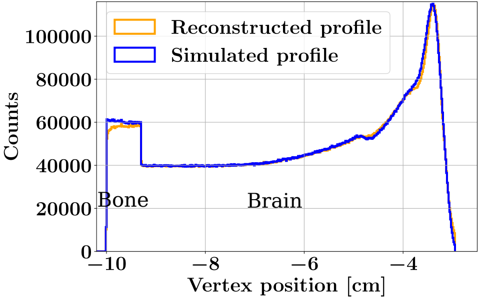

Two main reconstruction discrepancies:
specific uncorrelated PG-rays

Validation of PGTI reconstruction method, assuming minor differences are negligible with realistic detector resolutions

Detection of a longitudinal shift

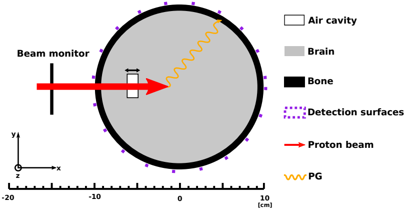

Simulation parameters

- **Air cavity** of variable thickness (1 to 1.5 cm)
- 30 detection surfaces of $\mathbf{1\times1\ cm^2}$ with **100 ps rms**, **1 MeV rms**, and a detection efficiency of **25 %**
- **6 mm rms** wide proton beam with **0.1% FWTM** of energy spread

Detection of a longitudinal shift

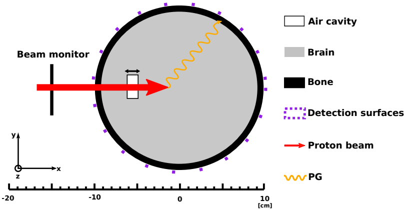

Simulation parameters

- **Air cavity** of variable thickness (1 to 1.5 cm)
- 30 detection surfaces of **1×1 cm^2** with **100 ps rms**, **1 MeV rms**, and a detection efficiency of **25 %**
- **6 mm rms** wide proton beam with **0.1% FWTM** of energy spread

Comparison of:

- **Irradiation reference profile** (1 cm air cavity, 1.5×10^9 impinging protons)
- **Treatment profile** (variable air cavity, 10^8 impinging protons)

Detection of a longitudinal shift

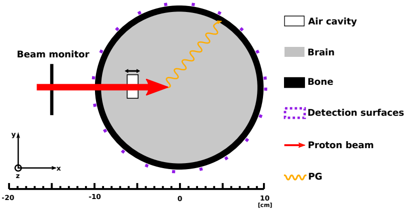

Simulation parameters

- **Air cavity** of variable thickness (1 to 1.5 cm)
- 30 detection surfaces of $\mathbf{1 \times 1}$ **cm**^{2} with **100 ps rms**, **1 MeV rms**, and a detection efficiency of **25 %**
- **6 mm rms** wide proton beam with **0.1% FWTM** of energy spread

Comparison of:

- **Irradiation reference profile** (1 cm air cavity, 1.5×10^9 impinging protons)
- **Treatment profile** (variable air cavity, 10^8 impinging protons)

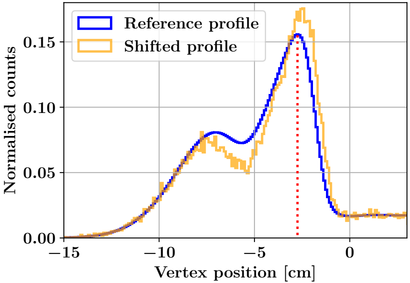

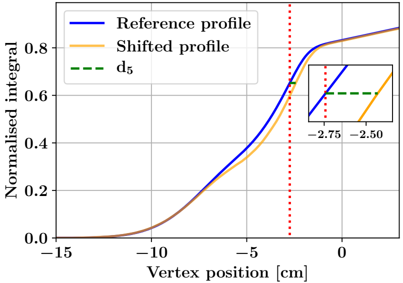

Detection of a transverse shift

Center Of Gravity (COG) method:

$$\boxed{\mathbf{r}_{COG} = \frac{1}{N}\sum_{i=0}^{N_{Det}} \mathbf{r}_i n_i}$$

Variables

- N: Total number of counts
- $\mathbf{r}_i$: i^{th} detector coordinate vector
- n_i: Number of counts in the i^{th} detector

Detection of a transverse shift

Center Of Gravity (COG) method:

$$\mathbf{r}_{COG} = \frac{1}{N}\sum_{i=0}^{N_{Det}} \mathbf{r}_i n_i$$

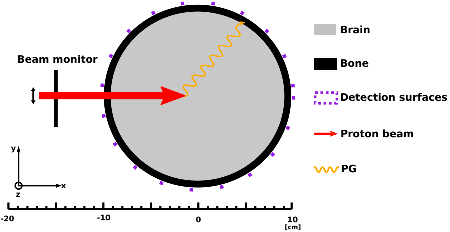

Variables

- N: Total number of counts
- $\mathbf{r}_i$: ith detector coordinate vector
- n_i: Number of counts in the ith detector

Simulation parameters

- **Y-shift** of the proton beam (0 to 0.5 cm)
- 30 detection surfaces of **1**$\times$**1 cm^2** with **100 ps rms**, **1 MeV rms**, and a detection efficiency of **25 %**
- **6 mm rms** wide proton beam with **0.1% FWTM** of energy spread

Detection of a transverse shift

Center Of Gravity (COG) method:

$$\mathbf{r}_{COG} = \frac{1}{N}\sum_{i=0}^{N_{Det}} \mathbf{r}_i n_i$$

Variables

- N: Total number of counts
- $\mathbf{r}_i$: ith detector coordinate vector
- n$_i$: Number of counts in the ith detector

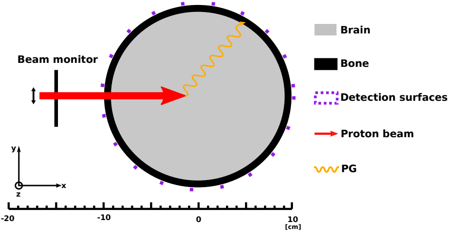

Simulation parameters

- **Y-shift** of the proton beam (0 to 0.5 cm)
- 30 detection surfaces of **1×1 cm^2** with **100 ps rms**, **1 MeV rms**, and a detection efficiency of **25 %**
- **6 mm rms** wide proton beam with **0.1% FWTM** of energy spread

Comparison of:

- **Reference COG** calculation (beam on the X-axis, 1.5×10^9 impinging protons)
- **Treatment COG** calculation (Y-shifted beam, 10^8 impinging protons)

Results

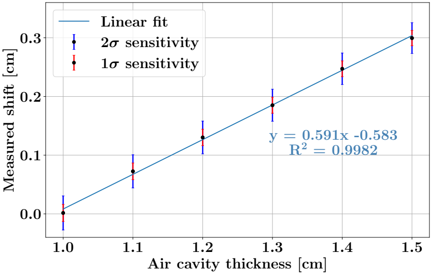

Longitudinal sensitivity

- **1 mm detection** of a beam shift at 2σ
- Linear behavior → **calibration**
- Fit slope < 1

Results

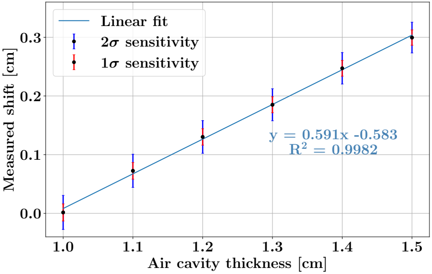

Longitudinal sensitivity

- **1 mm detection** of a beam shift at 2σ
- Linear behavior → **calibration**
- Fit slope < 1

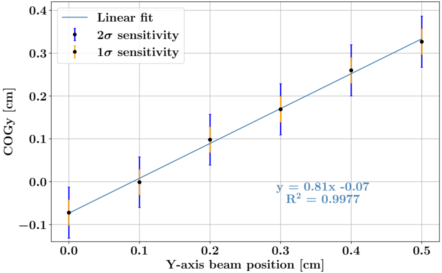

Transverse sensitivity

- **2 mm detection** of a beam shift at 2σ
- Linear behavior → **calibration**
- Fit slope < 1

Summary of PGTI results

	Longitudinal shift			Transverse shift
Number of protons	10^8	10^9	10^8	10^8
Methods	100 ps VR	1 ns VR	x_{COG}	y_{COG}
Sensitivity at 1σ (mm)	1	1	2	1
Sensitivity at 2σ (mm)	**1**	2	4	**2**

Detection of :

- **1 mm** of longitudinal beam shift at **2**σ on the **first irradiation spot**
- **2 mm** of transverse beam displacement at **2**σ on the **first irradiation spot**

Jacquet *et al* arXiv:2012.09275 submitted to Phys. Med. Biol, under revision

In progress :

- **3D reconstruction** (CPPM post-doc)

NB: A **very poor energy resolution** is enough to get those sensitivities

1 Introduction

2 New imaging modality: Prompt Gamma Time Imaging

3 Conception of TIARA detection system
- Crystal optimization
- Photodetector characterization

4 Conclusion

PGTI detection: Crystal

Ideal crystal: **fast and dense**

	Scintillators	Cerenkov radiators
Energy resolution	+	-
Time resolution	+	++
Density	+	++

PGTI detection: Crystal

Ideal crystal: **fast and dense**

	Scintillators	Cerenkov radiators
Energy resolution	+	-
Time resolution	+	++
Density	+	++

Optimization of a **Cerenkov detector**:

- Geometry
- Coating
- Photodetector
- Crystal type
- Optical coupling

Coating	**Black painting**	**Teflon**
Features	absorption	reflection
Energy resolution	- -	-
Time resolution	++	+
Detection efficiency	-	++

Optical coating simulations

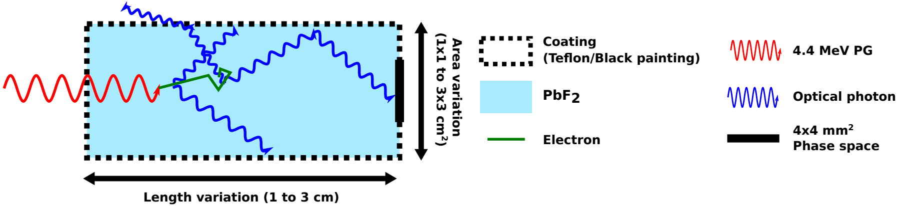

Optical coating simulations

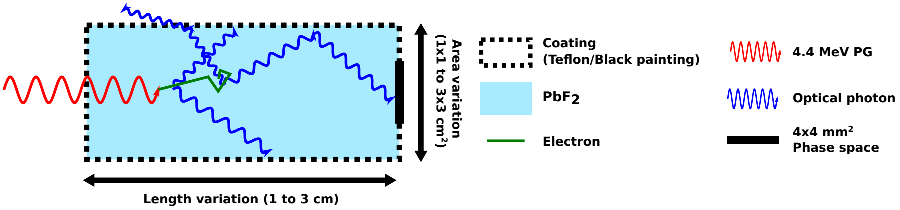

Criteria under studies

Energy resolution: deposited energy in a 1 cm^3 PbF_2 crystal for a 4.4 MeV PG

Time resolution: rms of 1^{st} optical photon TOF distribution

Detection efficiency $= \varepsilon_{geo} \times P_{int} \times P_{opt} \times PDE$

- ε_{geo}: geometrical efficiency
- P_{int}: probability of a 4.4 MeV PG interaction
- P_{opt}: probability to detect at least 2 Cerenkov photons
- PDE: probability of optical photon detection

Teflon coating optimization

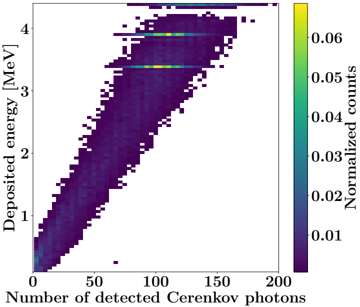

Optimization of a black painting-coated PbF_2

- Correlation deposited energy/detected Cerenkov

Teflon coating optimization

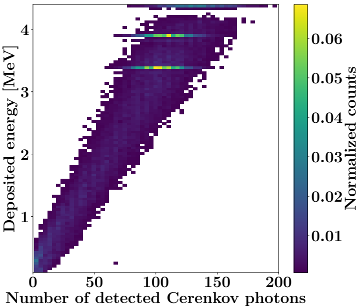

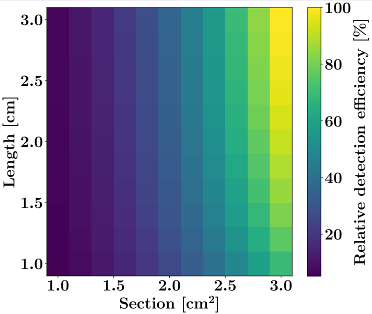

Optimization of a black painting-coated PbF_2

- Correlation deposited energy/detected Cerenkov
- Proportional increase of efficiency

Teflon coating optimization

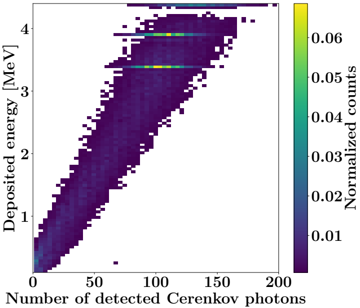

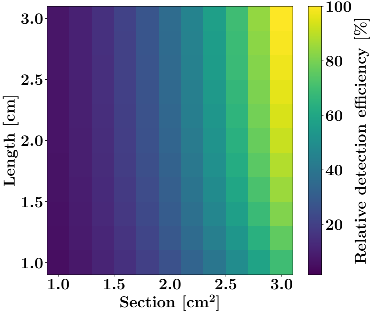

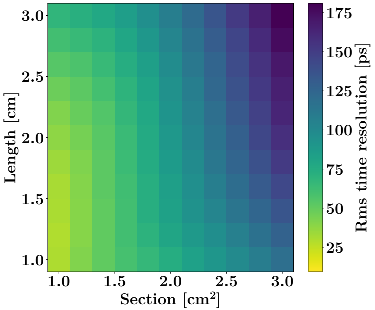

Optimization of a black painting-coated PbF_2

- Correlation deposited energy/detected Cerenkov
- Proportional increase of efficiency
- **Long crystal of small section**

Black painting coating optimization

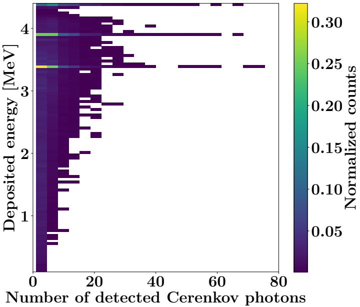

Optimization of a black painting-coated PbF_2

- No correlation deposited energy/detected Cerenkov

Black painting coating optimization

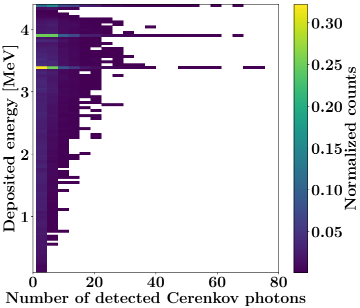

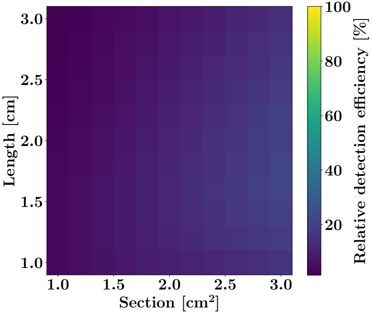

Optimization of a black painting-coated PbF_2

- No correlation deposited energy/detected Cerenkov

Black painting coating optimization

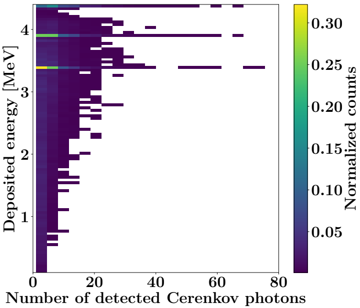

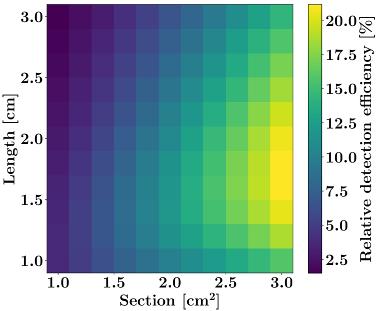

Optimization of a black painting-coated PbF_2

- No correlation deposited energy/detected Cerenkov
- **Short crystal of big section**

Black painting coating optimization

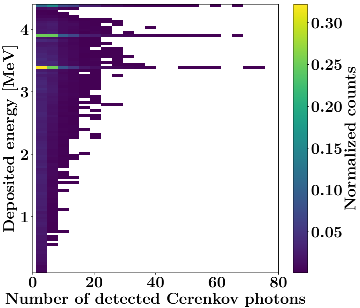

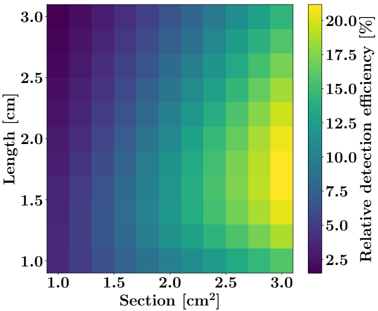

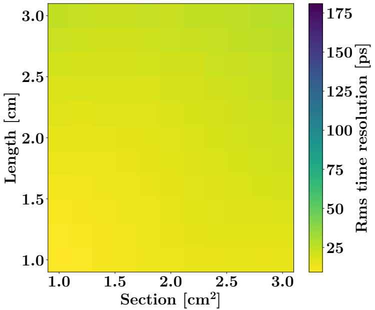

Optimization of a black painting-coated PbF_2

- No correlation deposited energy/detected Cerenkov
- **Short crystal of big section**
- Excellent time resolution

1. Introduction

2. New imaging modality: Prompt Gamma Time Imaging

3. Conception of TIARA detection system
   - Crystal optimization
   - Photodetector characterization

4. Conclusion

Photodetection: Silicon Photo Multiplier (SiPM)

SiPM: SPAD in parallel mode

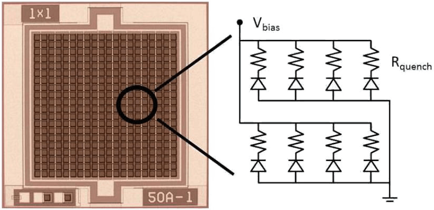

SiPM characterization

- **Breakdown Voltage** (BV) estimation
  ⇒ SiPM working in Geiger-mode
- **OverVoltage** (OV)= Bias Voltage - BV
  ⇒ OV optimization: Improvement of the SiPM **time resolution**

Photon counting mode

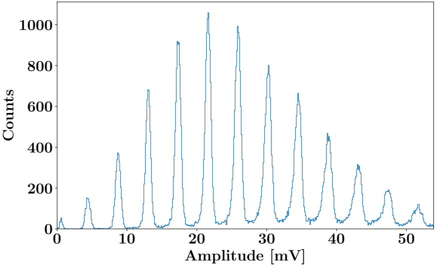

Typical IV curve

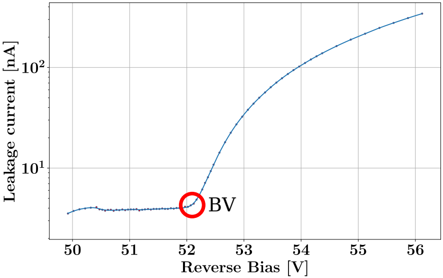

Photodetection: Silicon Photo Multiplier (SiPM)

SiPM: SPAD in parallel mode

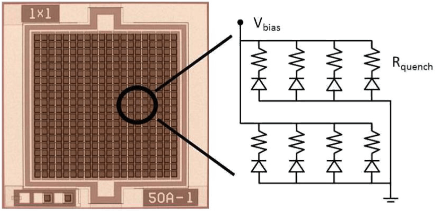

SiPM characterization

- **Breakdown Voltage** (BV) estimation
  $\Rightarrow$ SiPM working in Geiger-mode
- **OverVoltage** (OV)= Bias Voltage - BV
  $\Rightarrow$ OV optimization: Improvement of the SiPM **time resolution**

Photon counting mode

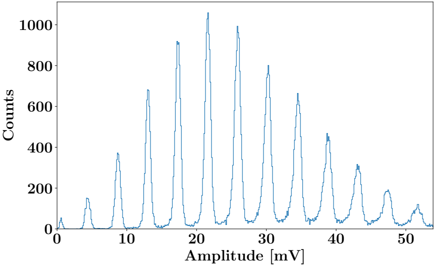

Typical IV curve

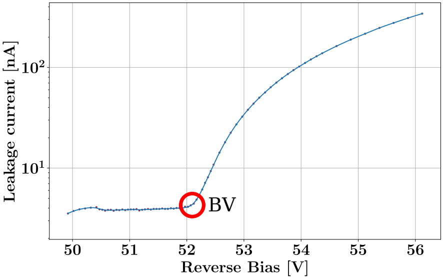

SiPM time resolution function of the number of detected optical photon

Experimental set-up

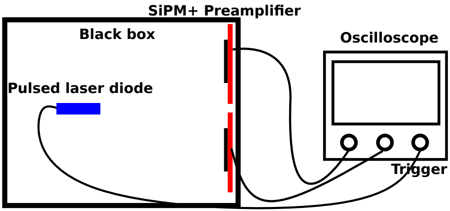

Experiment features

- Pulsed laser diode (14 ps rms)
- SiPM (Hamamatsu/FBK)
- Lecroy oscilloscope
  - 1GHz bandwidth
  - 100 ps sampling

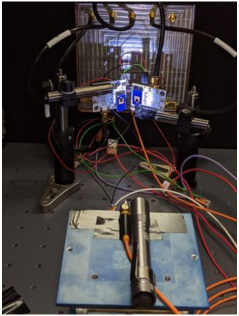

Experiment realised at the SDI

Experimental set-up

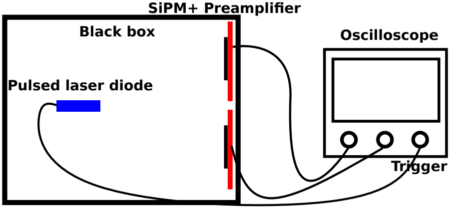

Experiment features

- Pulsed laser diode (14 ps rms)
- SiPM (Hamamatsu/FBK)
- Lecroy oscilloscope
  - 1GHz bandwidth
  - 100 ps sampling

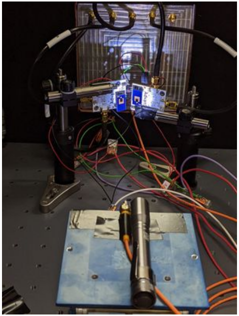

Experiment realised at the SDI

Measurement principle

Trigger on the diode pulse emission

- Measurement of a Δt between the 2 SiPM signals

$$\sigma^2_{\Delta t} = 2(\sigma^2{}_{\text{SiPM}} + \sigma^2{}_{\text{preamplifier}} + \sigma^2{}_{\text{laser}})$$

Assuming σ_{laser} negligible: $\sigma_{\Delta t} = \frac{\sigma_{\Delta t}}{\sqrt{2}}$

Results

OV optimization: Single Photon Time Resolution (SPTR) measurement

- Data selection: 1 photon for both SiPMs
- SPTR $\approx$ 100 - 150 ps rms

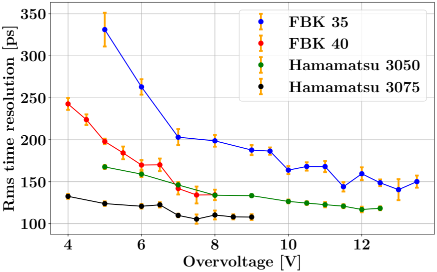

Results

OV optimization: Single Photon Time Resolution (SPTR) measurement

- Data selection: 1 photon for both SiPMs
- SPTR ≈ 100 - 150 ps rms

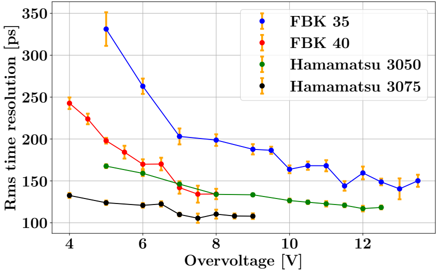

Time resolution function of number of detected photon (N_{photon}) measurement

- Calibration $N_{photon} = f(I_{laser})$
- Time resolution down to ≈ 30 - 40 ps rms

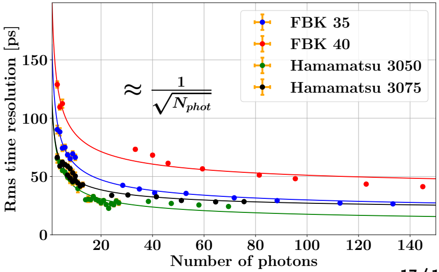

Detector development summary

Simulation: Measurement of the **crystal intrinsic time resolution** function of geometry and coating

Experiment: Determination of **photo detector time resolution** function of the number of detected photon

In progress:

Combination of experimental and simulation results

Assessment of other **crystal parameters**

- Crystal type ($PbWO_4$)
- Crystal/photo detector optical coupling

Cerenkov radiator/SiPM coupling and measurement of **the coincidence time resolution with a Co^{60}** source

Combination of crystal + photodetector to test under **proton beam**

1 Introduction

2 New imaging modality: Prompt Gamma Time Imaging

3 Conception of TIARA detection system
- Crystal optimization
- Photodetector characterization

4 Conclusion

Conclusion

Proof of concept of the PGTI potential in terms of sensitivity to longitudinal and transverse proton beam deviations

Preliminary characterization of the pixel design (simulations + laboratory experiments)

Perspectives

Beam Test (Centre Antoine Lacassagne/Arronax) to test different selected detector configurations

Global TIARA simulations including :

- Realistic detector design
- Realistic patient anatomy (voxelized images provided by the Centre Antoine Lacassagne)